

Extraction of Medically Interpretable Features for Classification of Malignancy in Breast Thermography

Himanshu Madhu, *Member, IEEE*, Siva Teja Kakileti, *Member, IEEE*, Krithika Venkataramani, *Member, IEEE* and Susmija Jabbireddy

Abstract— Thermography, with high-resolution cameras, is being re-investigated as a possible breast cancer screening imaging modality, as it does not have the harmful radiation effects of mammography. This paper focuses on automatic extraction of medically interpretable non-vascular thermal features. We design these features to differentiate malignancy from different non-malignancy conditions, including hormone sensitive tissues and certain benign conditions, which have an increased thermal response. These features increase the specificity for breast cancer screening, which had been a long known problem in thermographic screening, while retaining high sensitivity. These features are also agnostic to different cameras and resolutions (up to an extent). On a dataset of around 78 subjects with cancer and 187 subjects without cancer, that have some benign diseases and conditions with thermal responses, we are able to get around 99% specificity while having 100% sensitivity. This indicates a potential breakthrough in thermographic screening for breast cancer. This shows promise for undertaking a comparison to mammography with larger numbers of subjects with more data variations.

I. INTRODUCTION

As breast cancer is the most common cancer among women around the world [1], and early detection helps in better treatment, screening for breast cancer is useful. While mammography has been typically used for screening, it has disadvantages of low sensitivity for dense tissues and younger women, risk of causing breast cancer through the harmful radiation, and painful examination due to pressure involved in breast compression. Thermography is being re-considered as an alternative for breast cancer screening due to the advent of high resolution thermal cameras [2,3] and does not have these disadvantages as infra-red radiation emitted by the human body is used for screening and there is no contact. Breast cancer tumors are at a higher temperature due to increased metabolism [4] and hence can be detected by thermography.

Borchardt et al [5] provide a good survey of different algorithms in the literature [5] that detect breast cancer using thermography. These are mostly naïve approaches, using temperature features based on mean, standard deviation and other moments, or textural features based on Haralick descriptors including energy, entropy, contrast [6] or histogram based features for asymmetry analysis [7,8]. These features are classified using standard classification

algorithms such as Support Vector Machines, Neural Networks, etc. In [9], a Fractal Dimension (FD) based approach is used for classification of benign and malignancy based on the experimental evidence that malignant tumor boundaries are more irregular than benign tumors. They tested on a very small dataset of about three benign and three malignant samples, which is insufficient, and these results may not hold for larger datasets.

There are hardly any algorithms for cancer classification that are based on features that are medically interpretable [10]. While there are visual features used by thermographers [2-4, 11-12] that are clinically relevant, using abnormal focal increase in temperature and thermal patterns of the contralateral breasts, there is not much work on automatic extraction of such medical features. Classification using a comprehensive set of medically relevant thermographic features would also present biologically relevant information to the doctor for additional analysis. Additional analysis could involve other tests including a biopsy at the location of suspected malignancy, or treatment approaches for at-risk patients. One of the problems in thermography is low specificity at one sitting. Generally, benign conditions are determined by observing changes in thermal patterns after a few months in additional examinations.

In this paper, we propose novel approaches to extract features that have a medical significance and are easily interpretable by clinician, as well as improve specificity. We use a standard classifier ensemble on these features for classification. A detailed description of our dataset is provided in Section II. Section III and IV describes our proposed approach for feature extraction and classification, followed by Section V that gives the results of our proposed approach with comparison to existing algorithms.

II. DATASET DESCRIPTION

It is difficult to obtain large datasets in thermography for research purposes due to prior disadvantages of thermography of low specificity. Recent research has been conducted in datasets of an order of 100 subjects or less typically. We obtained an anonymized dataset of 265 subjects in India through our collaboration with a hospital at Manipal University and a clinic, which is a unit of Central Diagnostic Research Foundation. The Ethical Review Committee of both institutions approved all experimental procedures involving these subjects, and subject consent is taken to collect their data. The clinic uses thermography and sono-mammography for diagnosis. In the clinic, the subject is made to wait in an air-conditioned room for 15 minutes to suppress any external heat. Thermal images/videos of seated

Himanshu Madhu, Siva Teja Kakileti, Krithika Venkataramani are with Xerox Research Center India, Bangalore (phone: +91 8030461700; e-mail: Himanshu.Madhu2@xerox.com, SivaTeja.Kakileti@xerox.com, Krithika.Venkataramani@xerox.com). Susmija Jabbireddy is a dual degree B.Tech/M.Tech student at Indian Institute of Technology, Kharagpur.

subjects, with their hands raised upwards, were captured. From the clinic, a set of five thermal images comprising of frontal, left & right lateral and oblique views were captured using the Meditherm IRIS2000 camera with a resolution of 320 x 240 pixels, for 200 subjects. From the hospital, we captured thermal videos of 65 subjects with biopsy confirmed breast cancer, out of which, the initial 20 subjects were captured using FLIR E60 camera with resolution of 320 x 240 pixels and the remaining were captured using FLIR T650SC with resolution of 640 x 480 pixels. Among these subjects, 11 subjects have tumor size less than 2cm (T1), 41 subjects have tumor size from 2-5cm (T2), 9 subjects have tumor size greater than 5cm (T3) and 4 subjects have tumor touching skin or chest wall (T4) [13]. Fifteen subjects had deep tumors. We manually extracted frames corresponding to the five views from these thermal videos, to bring in uniformity of images from both datasets.

The ground truth labels for the clinic dataset is the doctor's conclusion based on sono-mammography and thermography reports along with confirmation from biopsy reports of suspicious cases for cancer, whereas the ground truth for the hospital dataset is based on mammography, sono-mammography, biopsy and surgery reports, where available. The entire dataset from the hospital and the clinic is in the age group of 19 to 82 years old and consists of 120 normal subjects, 53 subjects with benign conditions, 8 non-malignant cases with hormone sensitive tissues, 6 lactating mothers and 78 subjects with malignancy. Fig. 1 shows sample images of a normal subject, and subjects with a benign tumor, hormone sensitive tissues without malignancy, lactating conditions, and a malignant tumor.

III. PROPOSED FEATURE EXTRACTION ALGORITHM

Most of the approaches proposed in the literature [3-6, 8] extract features from the entire region of interest (ROI). Instead of extracting features from the entire ROI, our proposed approach extracts features from the abnormal regions detected within the ROI. An abnormal region is a subset of the ROI that shows a significant increase in temperature as compared to the neighboring areas [13]. These abnormal regions are further divided into hot spots and warm spots based on the degree of their thermal response.

A. Detection of Hot-spots and Warm-spots

Hot spots correspond to high temperature regions segmented using a combination of temperature-based features proposed in [13]. These temperature thresholds for segmentation, T_1 and T_2 , are defined by Eq. (1) and (2) below.

$$T_1 = \mu + \rho * (T_{max} - \mu) \quad (1)$$

$$T_2 = T_{max} - \tau \quad (2)$$

where μ refers to the mean of the modes of the ROI temperature histograms in all views, T_{max} represents the overall maximum temperature in all views, ρ represents the fraction of increase of T_1 over μ , and τ represents the reduction in temperature of T_2 from T_{max} . Warm spots correspond to slightly lower temperature regions as compared to hot spots, and have different parameters. This further division of warm-spots plays a part in detection of deep

tumors as well as in intra-class classification of non-malignant categories such as benign conditions, hormone sensitive tissues and extraneous heat. We select the parameters, ρ and τ , to improve classification, using a cross-validation set, as described below.

Selection of Parameters using a classification algorithm: As the extracted hot spots/warm spots play a major role in the sensitivity and specificity of the classification algorithm, we choose the parameters, ρ and τ , that maximize the linear combination of sensitivity and specificity as in Eq. (3).

$$J = \text{Sensitivity} + \lambda * \text{Specificity} \quad (3)$$

B. Feature Extraction

We detect hot spots and warm spots in each view and ROI, and extract features from them, as defined here and summarized in Table I. We define the best view as the view in which the size of the detected abnormal region, normalized with respect to the ROI, is maximum. From the detected hot spots in multiple views, we use the hot spots from the best view only to extract the hot-spot features. However, we use the warm spots from the best view and its contralateral-side view, to extract the warm spot features, due to which the warm spot features are more. This helps in determining the conditions that affect low heat rise in both sides.

1) *Presence of Abnormal Regions:* As a measure of thermal abnormality, we include the number of hotspots in the best view, the number of warm spots in the best view & contralateral-side view, and their area, normalized with respect to the ROI, in our feature set.

2) *Relative Temperature:* It is experimentally observed using contact temperature measurements [4] that the malignant tumor is hotter than its surrounding tissues. Gautherie [4] stated that the high metabolic activity of the cancerous cells leads to its increase in temperature. We calculate the mean temperature difference between the detected hot spot/warm spot and the remaining ROI and use this as a feature.

3) *Thermal Comparison of Contralateral Breasts:* In case of malignant tumors, certain benign tumors, inflammation or wound-healing cases, an increase in temperature in the abnormal regions is observed [2-3, 11-12, 14]. This leads to an asymmetry in thermal patterns compared to the contralateral breasts. However, similarity in thermal patterns is seen in both breasts for normal, hormone sensitive tissues and lactating conditions [2], due to the presence of similar hormone sensitive tissues in both breasts. We capture this property in our approach by using the following features.

a) *Mirror Overlap Area:* This feature shows how symmetrical is the temperature distribution on contralateral breasts. We create binary images corresponding to the abnormal regions, on the best view and its contralateral-side view. We compute the area of mirror overlap by finding the maximum of the convolution between the binary images of the two sides, and normalize it using the area of the ROIs.

b) *Area Difference:* We use this in conjunction with the above feature. It is computed as the normalized difference in the abnormal region areas between each view and its contralateral view, found for the three views separately.

TABLE I: PROPOSED FEATURES

Properties	Features Extracted	Hot spot features count	Warm spot features count
Boundary Features	Deviation from Circle and Ellipse, Irregularity and Fractal Dimensionality.	4	8
Thermal Comparison of Contralateral Breasts	Mirror Overlap, Thermal Distribution Ratio and Area Difference.	5	5
Relative Temperature	Relative Temperature to surrounding tissues	1	2
Presence of Abnormal Regions	Number and Size	2	4

c) *Thermal Distribution Ratio*: Though there is a similarity in thermal patterns for hormone sensitive tissues, we observed that it might not be an exact mirror symmetry. Hence, the relative areas of abnormal regions in both breasts is used as an additional feature. It is defined as the ratio of the hot spot/warm spot area in the contralateral-side view to the hot spot/warm spot area in the best view.

4) *Boundary*: Malignant tumor cells are aggressive in nature, due to which they invade surrounding tissues by rupturing through the boundary formed by basal laminas [15-16]. This makes the malignant tumor boundary irregular as compared to non-malignant cases like benign tumors whose cells behave similar to normal cells [15]. In [9], EtehadTayakol et al explored this behavior using fractal dimensions. In our approach, we analyzed this nature using the deviation of the boundary from regular shapes, as explained below.

a) *Deviation from Circle and Ellipse*: This shape-based feature uses the deviation of the detected hot spot/warm spot boundary from their best-fit circle and ellipse. We use convex optimization [17] to minimize the squared algebraic distance between the boundary of the detected hot spot/warm spot and its best-fit circle and ellipse function.

b) *Irregularity*: This feature is a slight modification to the above mentioned circle-deviation feature, and uses a circle that has a radius equal to the maximum distance from the centroid of the detected abnormal region to its boundary, as proposed in [18]. We calculate this feature using Eq. (4).

$$I(R) = \frac{1 + \sqrt{\pi} \max_{i \in R} \sqrt{(x_i - \bar{x})^2 + (y_i - \bar{y})^2}}{\sqrt{N(R)}} - 1 \quad (4)$$

where R represents a detected abnormal region, $N(R)$ represents the area of R , (x_i, y_i) and (\bar{x}, \bar{y}) represent the i^{th} point on R and the centroid of R , respectively.

c) *Fractal Dimensionality*: In [9, 19], fractal dimension

TABLE II: TEST SET RESULTS USING DIFFERENT CLASSIFIERS

	Sensitivity (%)	Specificity (%)
Our approach - Random Forests	100	98.9
Our approach - SVM	90	94.3
Textural Features from [6]	57.5	73.0

of all hotter regions, extracted using Fuzzy C-means, is used as a measure for irregular boundaries. In our approach, we compute the fractal dimension of each abnormal region extracted as mentioned in Section IIIA, and we use the maximum fractal dimension among these as our feature.

IV. CLASSIFICATION

In our work, we tested our data set with standard classifiers such as Support Vector Machines (SVM), and Random Forests (RF), an ensemble of decision tree classifiers. The RF randomly picks subsets of the training subjects and feature subsets into groups, and within each group, a decision tree is trained. For a test subject, the mode of the decisions of these randomly generated trees is used for classification. We found that the RF performs better compared to SVM on our dataset, probably because our features are better suited to decision trees, and ensemble fusion is better than single classifiers.

V. EXPERIMENTATION

We manually cropped the thermal images obtained from the clinic and hospital to remove unwanted regions like the infra-mammary folds, axilla, sternum and other non-breast regions. We randomly selected 90 subjects from the entire dataset for training, with 27 normal, 25 benign, 3 with hormone sensitive tissues, 2 lactating and 33 malignant cases. The remaining dataset was divided into cross-validation and test sets with a size ratio of 1:2, respectively. A RF with 100 trees or SVM was trained using this training set for 2-class classification. We use the cross-validation set to find the optimal values for the parameters (ρ, τ) of hot spots and warm spots that maximize J , as mentioned in Section III using a step size of $(0.1, 0.2^\circ\text{C})$. Since sensitivity is more important for cancer screening, we choose λ to be 0.5. To find μ , a histogram bin width of 0.5°C is chosen for uniformity, as the clinic data had this temperature sensitivity. As there is randomness in the RF ensembles, we used the maximum of average J in 20 iterations of RFs to find the optimal values of (ρ, τ) , which are $(0.5, 1.4^\circ\text{C})$ and $(-0.1, 2.6^\circ\text{C})$ for hot spots and warm spots, respectively.

Table II shows the sensitivity/specificity of our features on the test set using RFs and SVMs. We are able to detect all the deep malignant tumors using this approach unlike in [13], and improve specificity over approaches using just hot spot detection [20] by correctly determining the non-

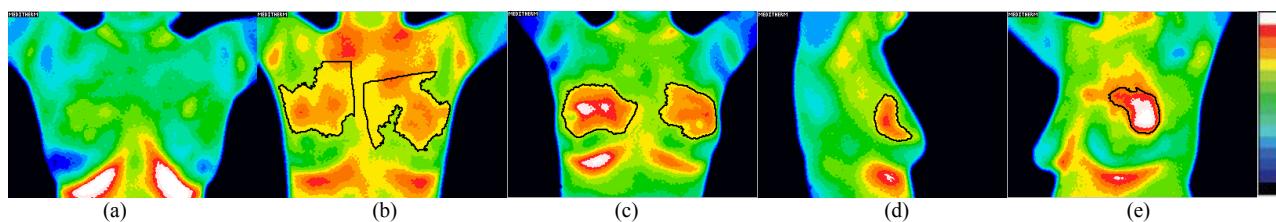


Figure 1. Sample Subject Images for (a) Normal case in frontal view, (b) Hormone sensitive tissues showing warm-spots in frontal view, (c) Lactating case showing warm-spots in frontal view, (d) Benign case showing warm-spots in right lateral view and (e) Malignant case showing hot-spots in left oblique view. The color-bar shows increasing temperature in 0.5°C gradations with white being the highest temperature.

malignant categories that have a thermal response. We implemented the textural feature algorithm given in [6] on our dataset and the results on the combined test and cross-validation sets (as no parameter tuning is required here) are given in Table II. The algorithm proposed in [9] using fractal dimension resulted in very low sensitivity values on our dataset. The obtained sensitivity and specificity using our approach is very high compared to other thermographer based [2-4, 11-12] and image processing based algorithms [5-10, 13, 20] on a dataset greater than 100 subjects.

VI. CONCLUSIONS AND FUTURE WORK

The classification of malignancy from non-malignancy is a difficult problem in thermography if the temperature increases alone (hot spots/ warm spots) are considered, since there are non-malignant conditions having temperature increases, such as lactating conditions, hormone sensitive tissues, and some benign conditions that show temperature rises at times. However, by using properties of hot spots and warm spots, unlike other algorithms that use the entire ROI, this classification can become easier, as shown in our approach. Due to the differences in these properties for malignancy and non-malignancy, e.g. more irregular boundaries in malignancy, and more symmetry in size and number of warm-spots for non-malignancy, these features are significantly able to provide better classification. Classifier ensembles, rather than single classifiers, play a lesser role than these features, in improving classification. We plan to analyse the role of different features, ensembles and type of base classifiers, along with their effect on the various sub-categories in a future work, to explain further the reasons for the higher specificity and sensitivity. The high specificity achieved here enables thermographic screening in one sitting, unlike prior thermography approaches requiring multiple sittings, which is an important advance. We also plan evaluation on larger datasets with more data variations.

ACKNOWLEDGMENT

We thank Dr. H. V. Ramprakash of Central Diagnostic Research Foundation, Dr. L. Ramachandra, Dr. S. S. Prasad, and Dr. Vijay Kumar of Manipal University, and their staff, in aiding us by providing data and giving medical insights.

REFERENCES

[1] C. Fitzmaurice, et al., "The global burden of cancer 2013," *JAMA oncology*, vol. 1, no. 4, pp. 505-527, 2015.

[2] D. A. Kennedy, T. Lee and D. Seely, "A comparative review of thermography as a breast cancer screening technique," *Integrative Cancer Therapies*, vol. 8, no. 1, pp. 9-16, 2009.

[3] J. R. Keyserlingk, P. D. Ahlgren, E. Yu, N. Belliveau and M. Yassa, "Functional infrared imaging of the breast," *IEEE Engineering in Medicine and Biology Magazine*, vol. 19, no. 3, pp. 30-41, 2000.

[4] M. Gautherie, "Thermobiological assessment of benign and malignant breast diseases," *Am. J. Obstet. Gynecol.*, vol. 8, no. 147, pp. 861-869, 1983.

[5] T. B. Borchardt, A. Conci, R. C. F. Lima, R. Resmini and A. Sanchez, "Breast thermography from an image processing viewpoint: A survey," *Signal Processing*, vol. 93, no. 10, pp 2785-2803, 2013.

[6] U. R. Acharya, E. Y. K. Ng, J. Tan, and S. V. Sree, "Thermography based breast cancer detection using texture features and support vector machine," *Journal of Medical Systems*, vol. 36, no. 3, pp. 1503-1510, 2012.

[7] P. T. Kuruganti and H. Qi, "Asymmetry analysis in breast cancer detection using thermal infrared images," in *Proc. Second Joint IEEE EMBS/BMES Conf.*, vol. 2, 2002, pp. 1155-1156.

[8] X. Tang, and H. Ding, "Asymmetry analysis of breast thermograms with morphological image segmentation," in *Proc. 27th Annu. Int. Conf. IEEE Engineering in Medicine and Biology Society (EMBS)*, 2006, pp. 1680-1683.

[9] M. EtehadTayakol, C. Lucas, S. Sadri and E. Y. K. Ng, "Analysis of breast thermography using fractal dimension to establish possible difference between malignant and benign patterns" *Journal of Healthcare Engineering*, vol. 1, pp. 27-43, 2010.

[10] J. E. Goin and J. D. Haberman, "Automated breast cancer detection by thermography: Performance goal and diagnostic feature identification," *Pattern Recognition*, vol. 16, no. 2, pp. 125-129, 1983.

[11] M. Gautherie, "Improved system for the objective evaluation of breast thermograms," *Progress in Clinical and Biological Research*, vol. 107, pp. 897-905, 1981.

[12] M. Gautherie and M. C. Gros, "Breast thermography and cancer risk prediction," *Cancer*, vol. 45, no. 1, pp. 51-56, 1980.

[13] K. Venkataramani, L. K. Mestha, L. Ramachandra, S. S. Prasad, V. Kumar and P. J. Raja, "Semi-automated breast cancer tumor detection with thermographic video imaging," in *Proc. 37th Annu. Int. Conf. IEEE EMBS*, 2015, pp. 2022-2025.

[14] W. F. Ganong, *Review of Medical Physiology*. New York: McGraw-Hill, ED-22, 2005.

[15] H. Lodish, A. Berk, S. L. Zipursky, P. Matsudaira, D. Baltimore and J. Darnell, *Tumor cells and the onset of cancer*. New York: W. H. Freeman and Company, Molecular cell biology, ED - 4, 2000.

[16] J. W. Baish and R. K. Jain, "Fractals and Cancer," *Cancer Research*, vol. 60, no. 14, pp. 3683-3688, 2000.

[17] A. Fitzgibbon, et al., "Direct least square fitting of ellipses," *IEEE Trans. PAMI*, vol. 21, no. 5, pp. 476-480, 1999.

[18] M. Nixon, *Feature extraction & image processing*. Academic Press, 2008.

[19] B. B. Mandelbrot, *The fractal geometry of nature*. San Francisco: W. H. Freeman, 1983.

[20] K. Venkataramani, H. Madhu, S. Sharma, H. V. Ramprakash, A. Rajendra, A. K. Parthasarathy, G. Manjunath and L.K. Mestha, "Initial evaluation of semi-automated breast cancer screening using thermography," in *Proc. Quantitative InfraRed Thermography Asia Conf.*, 2015.